paucity of objective data regarding the phenotypes and direction of differentiation of the mucinous epithelium of IMBTs and EMBTs is another reason.

Distinction between IMBTs and EMBTs is important because their clinicopathological features differ significantly.[2,3,7,9–11] IMBTs comprise approximately 85% of MBTs. They are usually unilateral (more than 90%).[10] Most IMBTs are large multicystic masses, and their epithelial component has been described as a mixture of intestinal-, gastric- and endocervical-type mucinous epithelium that grows predominantly in glandular or cystic structures admixed with papillary and villous structures.[7,9,10] Although intestinal differentiation, which is represented by the presence of goblet cells and CDX2 immunoreactivity, has been regarded as a key feature of IMBTs,[2,7,9,10,12] mucinous epithelium that resembles gastric foveolar-type epithelium is often the predominant component of IMBTs in observations by ourselves and others.[2,13] In fact, Ji *et al.*[14] have reported frequent expression of MUC5AC, a gastric foveolar epithelial marker, in IMBTs. The tumour cells of IMBTs show a variable degree (mild to moderate) of atypia, and coexistence of a benign-looking mucinous cystadenoma component is often observed. It is generally accepted that stepwise malignant transformation occurs from mucinous cystadenoma to IMBT to usual type (non-endocervical type) mucinous adenocarcinoma. However, the precise origin of these tumours remains unclear.

Compared with IMBTs, EMBTs are much less common and smaller, and tend to occur in younger females.[15–17] EMBTs are more frequently bilateral, and show a paucilocular gross appearance with intracystic papillary projection.[11,17] Histologically, EMBTs are characterized by finely branching papillae with fibrovascular cores, and their architecture resembles closely that of serous borderline tumours (SBTs). The lining epithelium is composed of columnar mucin-containing cells (which resemble endocervical cells), and polygonal cells with eosinophilic cytoplasm.[9,11,18] However, the glandular epithelium of EMBTs does not necessarily resemble that of typical endocervical glands because the above two types of cells are usually admixed with each other, and cellular tufting and budding are prominent. Goblet cells are found rarely in EMBTs.[9,16,17] EMBTs are associated frequently with endometriosis,[15,16,19] and share common immunohistochemical features with SBTs and low-grade endometrioid carcinomas, such as positivity for oestrogen receptor (ER) and progesterone receptor (PgR), suggesting the Müllerian nature of the neoplasm.[2,3,5,8]

In this study, we have attempted to clarify the phenotypes and directions of differentiation of the mucinous epithelium that constitutes IMBTs and EMBTs by immunohistochemical analysis. A panel of antibodies that included gastric markers [claudin-18 (CLDN18), MUC5AC and MUC6], intestinal markers (MUC2 and CDX2), Müllerian markers (ER, PgR, CA125 and vimentin) and cytokeratins (CK7 and CK20) was applied. The expression of these markers was also assessed in SBTs to reveal the typical phenotype of Müllerian-type tumours. In this study, special attention was paid to the expression of CLDN18, which is a recently established gastric marker. CLDN18 is one of the claudins, a family of 27 proteins essential for the formation of tight junctions and the maintenance of polarity in epithelial and endothelial cells.[20,21] Positive immunoreactivity for CLDN18 has been shown in all types of gastric epithelium (foveolar-type, pyloric-type and fundic-type).[22,23] Thus, we believe that CLDN18 is one of the best pan-gastric immunohistochemical markers available at this time.

Materials and methods

TISSUE SAMPLES

A total of 79 ovarian MBTs (54 IMBTs and 25 EMBTs) from 75 patients were retrieved from the archives of the Department of Pathology of the University of Tokyo Hospital. These included 54 cases of unilateral IMBT, 17 cases of unilateral EMBT, and four cases of bilateral EMBTs. Two of the IMBTs coexisted with mature cystic teratoma (MCT). The discrepancy between the number of IMBTs and EMBTs is due to the relative rarity of EMBTs. We included all EMBTs that were resected between 1989 and 2011. Because IMBTs during this period far outnumbered EMBTs we selected 54 cases randomly, which is a substantial number for comparative analysis. We also added 22 cases of SBT to the series. Haematoxylin and eosin (H&E)-stained slides of all cases were reviewed. Histological diagnosis was based on the most recent criteria of the WHO.

IMMUNOHISTOCHEMISTRY

All tissue samples were fixed in formalin and embedded in paraffin. For immunohistochemistry, we arranged all the MBTs and SBTs in tissue microarrays (TMAs) with duplicate 2-mm cores obtained from each tumour. For those EMBT cases with bilateral involvement, tumours in the right and left ovaries

were submitted separately. TMA sections were cut at 4-μm thickness.

Immunohistochemistry for CLDN18, MUC1, MUC2, MUC5AC, MUC6, CK7, CK20, CDX2, CA125, ER, PgR and vimentin were performed in all ovarian borderline tumours. Antibodies used in this study are detailed in Table 1. For all antibodies, immunostaining was performed according to standard techniques using an autostainer (BenchMark XT; Ventana Medical Systems, Inc., Tucson, AZ, USA). Immunoreactivity was interpreted based on the presence of cytoplasmic staining for CK7, CK20 and vimentin; nuclear staining for CDX2, ER and PgR; membranous staining (with or without cytoplasmic staining) for CA125; and luminal/apical or combined luminal and cytoplasmic staining for MUCs. CLDN18 expression was evaluated based on the existence of basolateral membrane staining. Evaluation of immunohistochemistry was performed by two authors (S.A.H. and D.M.), who specialize in gynaecological pathology. Immunohistochemical reactions were scored based on the percentage of positive cells and graded as 0 (totally negative), 1 + (1–4%), 2 + (5–14%), 3 + (15–49%) and 4 + (≥50%). The average tumour cell positivity in two TMA cores was calculated, and then a grade was given. Appropriate positive and negative controls were included.

Table 1. Antibodies used for immunohistochemistry

Antibody	Dilution	Clone	Manufacturer
CLDN18	1:1000	Poly	Zymed
MUC1	1:100	MA695	Novocastra
MUC2	1:20	Ccp58	Novocastra
MUC5AC	1:100	CLH2	Novocastra
MUC6	1:100	CLH5	Novocastra
CDX2	1:200	CDX2-88	Cell Marque
CK7	1:100	OV-TL12/30	DakoCytomation
CK20	1:100	Ks 20.8	Novocastra
ER	Prediluted	ER1D5	Ventana
PgR	Prediluted	A9621A	Ventana
CA125	1:200	Ov 185:1	Novocastra
Vimentin	1:1000	V9	DakoCytomation

CLDN18, claudin-18; CK7, cytokeratin 7; CK20, cytokeratin 20; ER, *oestrogen receptor*; PgR, *progesterone receptor*.

HIERARCHICAL CLUSTERING OF OVARIAN BORDERLINE TUMOURS ACCORDING TO THEIR IMMUNOPHENOTYPE

Unsupervised two-way hierarchical clustering was performed based on Euclid distances and average linkage clustering algorithms in sample directions and antibody directions using Cluster software version 3.0 (Stanford University, http://bonsai.ims.u-tokyo.ac.jp/~mdehoon/software/cluster/software.htm#ctv). All IMBTs, EMBTs and SBTs were included in the analysis. For the expression level of each protein, data on the percentage of positive cells detected by immunohistochemistry were used. A heat map was drawn using the Java TreeView software (Alok, http://jtreeview.sourceforge.net/).

STATISTICAL ANALYSIS

Statistical analysis was performed using Fisher's exact test. Statistical analyses were performed using StatView software version 5.0 (SAS Institute, Cary, NC, USA), and a value of $P < 0.05$ was considered statistically significant.

Results

IMMUNOHISTOCHEMICAL COMPARISON OF IMBT AND EMBT

To reveal the characteristics of the mucinous epithelia that comprise IMBT and EMBT, we initially analysed the expression of markers that are known to represent either gastric or intestinal differentiation. The results are shown in Table 2. Positive immunoreactivity for CLDN18, a pan-gastric marker, was observed in nearly all cases (98%) of IMBTs, whereas EMBTs were usually CLDN18-negative (Figure 1). CLDN18 stained more than 50% of the tumour cells (4+) in the majority of IMBTs (48 of 56 cases). Diffuse basolateral staining was detected, especially in IMBTs that comprised stratified columnar mucinous epithelium that resembled gastric foveolar-type epithelium. However, we also found CLDN18 positivity in the epithelium of IMBTs that contained scattered goblet cells. Almost all EMBTs were completely negative for CLDN18 with the exception of one case that revealed focal positivity.

In addition to CLDN18 expression, significant differences between IMBTs and EMBTs were found with regard to the expression of MUCs and CDX2 (Figure 2). MUC5AC, a gastric foveolar epithelial marker, was expressed more frequently in IMBTs (93%) than

Table 2. Claudin-18, MUCs, and CDX2 expression in intestinal-type and endocervical-like mucinous borderline tumours

	CLDN18		MUC1		MUC2		MUC5AC		MUC6		CDX2	
	IMBT	EMBT	IMBT	EMBT	IMBT	EMBT	IMBT	EMBT	IMBT	EMBT	IMBT	EMBT
–	1	24	30	0	36	24	4	7	42	19	28	25
1+	0	0	9	3	9	1	2	5	6	2	12	0
2+	1	1	7	4	6	0	5	9	5	4	7	0
3+	4	0	5	5	3	0	9	3	1	0	6	0
4+	48	0	3	13	0	0	34	1	0	0	1	0
Total	53/54 (98%)	1/25 (4%)	24/54 (44%)	25/25 (100%)	18/54 (33%)	1/25 (4%)	50/54 (93%)	18/25 (72%)	12/54 (22%)	6/25 (24%)	26/54 (48%)	0/25 (0%)
P	<0.0001		<0.0001		0.0042		0.0307		>0.9999		<0.0001	

in EMBTs (72%) ($P = 0.0307$). Further, most IMBTs showed 3 + and 4+ immunoreactivity for MUC5AC. In contrast, MUC5AC expression in EMBTs was usually focal (1+ and 2+) or negative. Markers of intestinal differentiation, such as MUC2 and CDX2, were expressed in fewer than half of IMBTs (33% and 48%, respectively). Expression of MUC2 and CDX2 in IMBT was usually focal and patchy (1+ and 2+), and diffuse (4+) immunoreactivity for these markers was found in only 3% and 5% of the cases. EMBTs were almost always negative for MUC2 and CDX2. MUC6, a marker for gastric pyloric gland-type epithelium, was negative in most IMBTs and EMBTs. MUC1 expression was seen more frequently in EMBTs (100%) compared with IMBTs (44%).

The expression of conventional markers, including CK7, CK20, ER, PgR, CA-125 and vimentin, was also evaluated in IMBTs and EMBTs. The results are shown in Table 3. In our series, all IMBTs and EMBTs expressed CK7. The remaining markers were expressed differentially in IMBTs and EMBTs ($P < 0.0001$). IMBTs are characterized roughly by a $CK20^+/ER^-/vimentin^-$ immunophenotype, whereas most EMBTs display a $CK20^-/ER^+/vimentin^+$ pattern (Figure 3). CK20 expression was observed in 80% of the IMBTs, and was of variable extent; EMBTs were almost always negative for CK20. Markers that were positive in all EMBTs included ER, vimentin and CA125. The expression of ER, vimentin and CA125 in IMBTs was less frequent (4%, 2% and 35%, respectively). Finally, PgR was another positive marker for EMBTs, but expression was slightly less frequent (80%) compared with that of ER, and ER staining tended to be more diffuse.

IMMUNOPHENOTYPE OF SBTS AND HIERARCHICAL CLUSTERING OF OVARIAN BORDERLINE TUMOURS

We performed immunohistochemistry for all markers listed above in 22 cases of SBT. The results are shown in Table 4. Our investigation revealed that all SBTs were negative for CLDN18. Markers commonly expressed in SBTs included MUC1, CK7, ER, CA125 and vimentin. The dendrogram depicted in Figure 4 is the result of hierarchical clustering of IMBTs, EMBTs and SBTs according to their immunoprofiles. This dendrogram shows the degree of relatedness between the protein expression patterns detected by the 12 antibodies across the 101 cases of ovarian borderline tumours, with short branches indicating a high degree of similarity in the staining pattern. In the dendrogram, IMBTs comprised a distinct group that was separate from the EMBT/SBT group. Based on

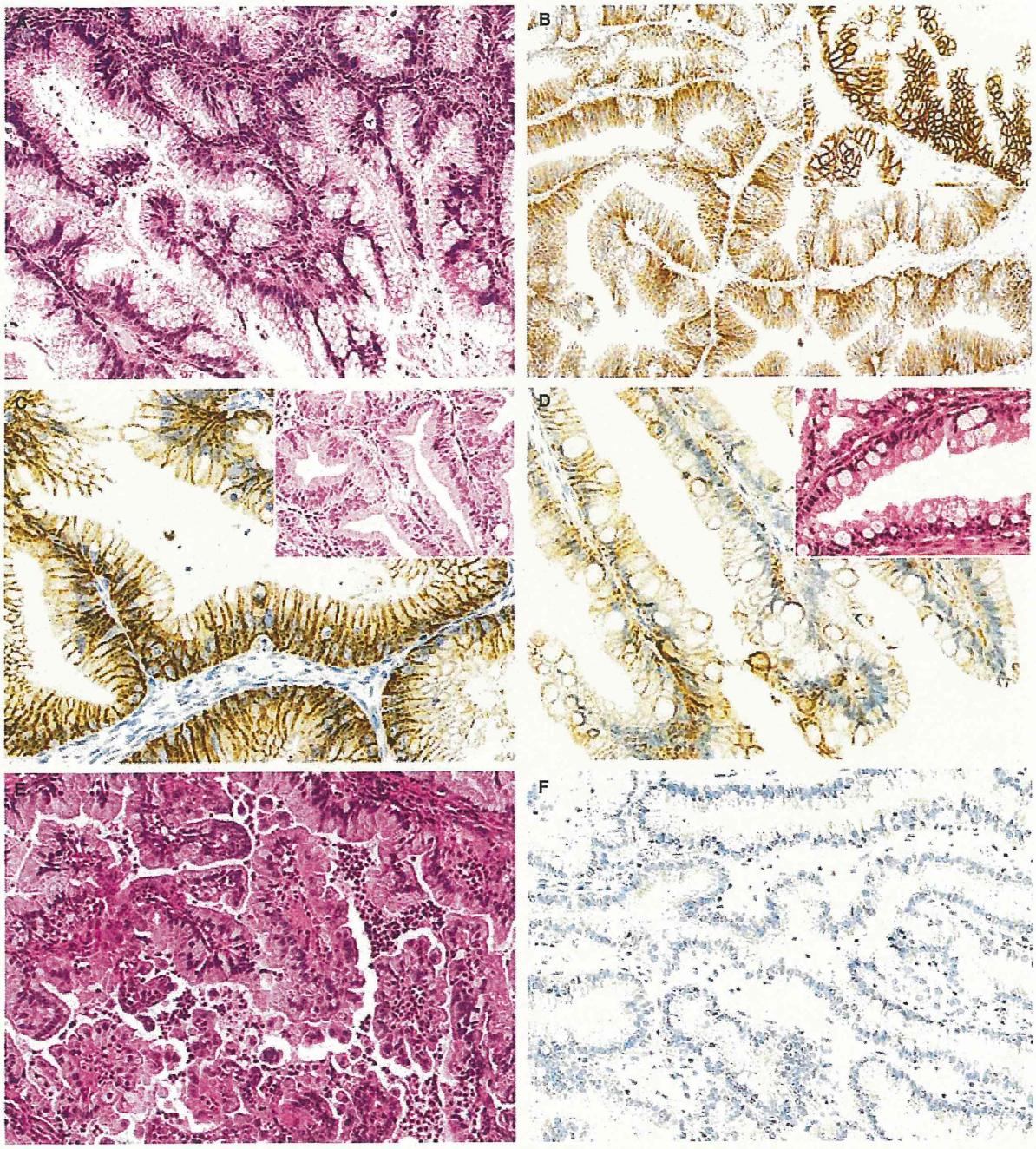

Figure 1. (A) Representative histology of intestinal-type mucinous borderline tumour (IMBT). (B) Diffuse membranous expression of CLDN18 in IMBT. (C) CLDN18 expression in gastric foveolar-type mucinous epithelium of IMBT. CLDN18 positivity is observed in the majority of the tumour cells. (D) Basolateral staining for CLDN18 is also observed in the Goblet cell-rich area of IMBT. (E) Representative histology of endocervical-like mucinous borderline tumour (EMBT) characterized by prominent papillary structures and stromal inflammation. (F) CLDN18 is completely negative in an EMBT.

the analyses of these 12 markers, EMBTs and SBTs were not clearly separated. Rather, similarities in the immunophenotypes of EMBTs and SBTs were highlighted in the dendrogram.

Discussion

Evidence of altered claudin expression in various human neoplasms has been accumulating rapidly.

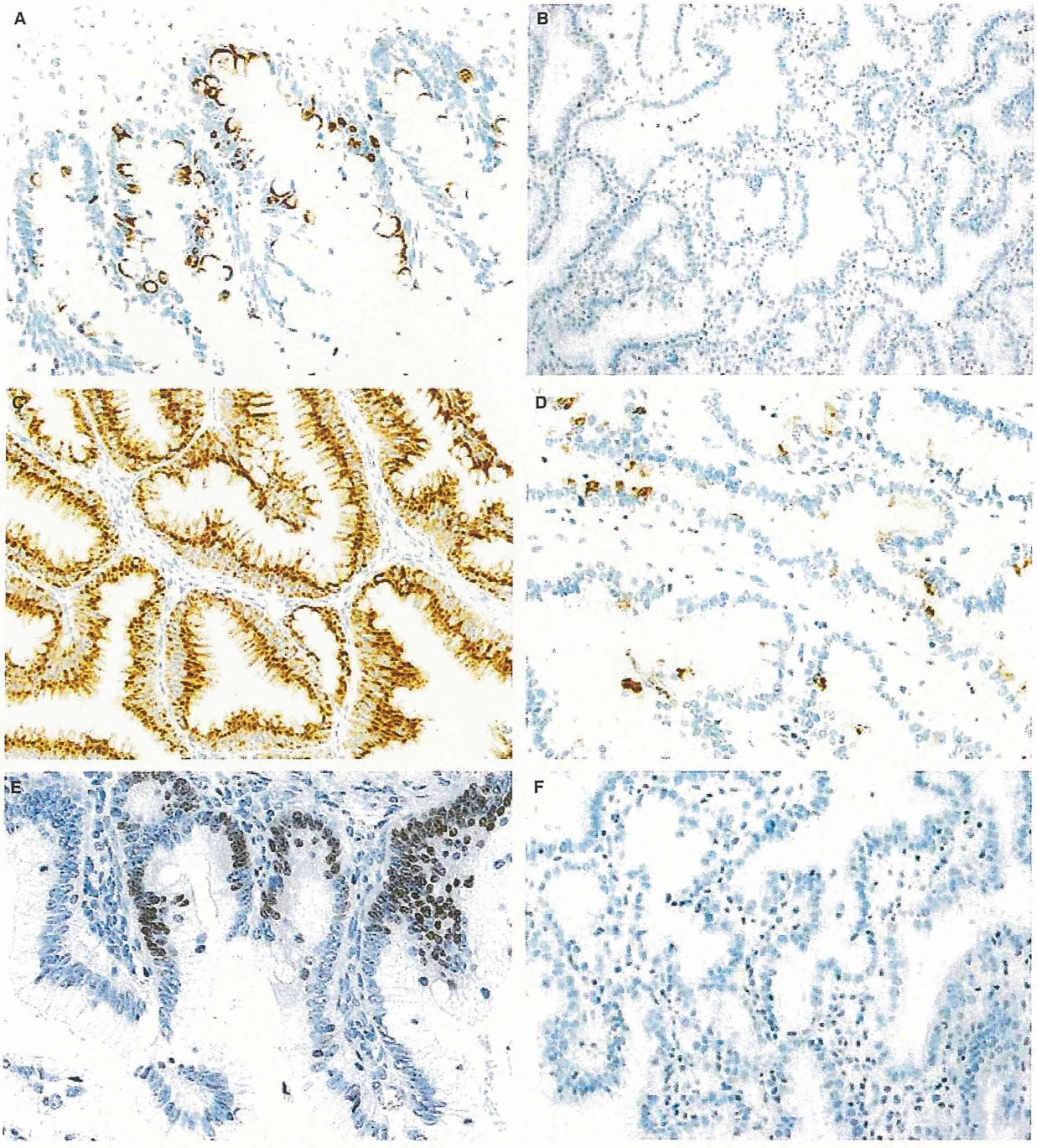

Figure 2. Expression of MUC2, MUC5AC and CDX2 in (A,C,E) intestinal-type mucinous borderline tumour (IMBT) and (B,D,F) endocervical-like mucinous borderline tumour (EMBT). (A) Focal MUC2 expression in a goblet cell-rich IMBT. (B) EMBT is negative for MUC2. (C) Diffuse MUC5AC expression in IMBT. (D) MUC5AC expression in EMBTs was often focal. (E) Patchy and focal CDX2 positivity in IMBT. (F) CDX2 was always negative in EMBTs.

Expression of CLDN18 has been studied in various types of human cancers and normal tissues.[23–31] Two alternatively spliced variants are present in mice: variant 1 (claudin18a1) is expressed in the lung, whereas variant 2 (claudin18a2) is expressed in the stomach.[27,29] In normal human tissues, expression of

Table 3. Expression of cytokeratins and Müllerian markers in intestinal-type and endocervical-like mucinous borderline tumours

	CK7		CK20		ER		PgR		CA125		Vimentin	
	IMBT	EMBT	IMBT	EMBT	IMBT	EMBT	IMBT	EMBT	IMBT	EMBT	IMBT	EMBT
–	0	0	11	24	52	0	53	5	35	0	53	0
1+	1	0	9	1	0	0	0	1	10	0	1	1
2+	2	0	10	0	2	0	1	6	4	0	0	2
3+	3	1	15	0	0	1	0	8	4	0	0	9
4+	48	24	9	0	0	24	0	5	1	25	0	13
Total	54/54 (100%)	25/25 (100%)	43/54 (80%)	1/25 (4%)	2/54 (4%)	25/25 (100%)	1/54 (2%)	20/25 (80%)	19/54 (35%)	25/25 (100%)	1/54 (2%)	25/25 (100%)
P	>0.9999		<0.0001		<0.0001		<0.0001		<0.0001		<0.0001	

claudin18a2 is confined to gastric epithelial cells (foveolar, endocrine, parietal and chief cells) and duodenal Paneth cells, and is not expressed in other organs, including the oesophagus, colon, pancreas and lung.[23,27,29,32] CLDN18 is now considered to be a highly selective immunohistochemical marker of gastric lineage, and its expression is considered to determine the gastric phenotype in neoplastic conditions.[24–26,31] Sanada *et al.*[29] used immunohistochemistry to reveal that CLDN18 is highly expressed in normal gastric cells and that its expression is retained in approximately half of gastric cancers. Interestingly, they showed further that CLDN18 is down-regulated in gastric epithelium with intestinal metaplasia and in gastric cancers with an intestinal phenotype. Our group showed recently that a subset of intrahepatic cholangiocarcinomas and pancreatic ductal carcinomas show a CLDN18-positive gastric phenotype.[24,25] It is of note that up-regulation of CLDN18 occurs in the early stage of cholangiocellular and pancreatic carcinogenesis, as shown by CLDN18 positivity in precancerous lesions such as pancreatic intraepithelial neoplasias and biliary intraepithelial neoplasias.

The current study is the first to investigate CLDN18 expression in ovarian borderline tumours. We demonstrated that the CLDN18-positive immunophenotype is observed specifically in IMBTs and not in EMBTs or SBTs. Another gastric marker, MUC5AC, which is expressed in normal gastric foveolar epithelium, was also expressed frequently in IMBTs, giving further support to the gastric differentiation of the IMBT epithelium. Because previous reports have shown that normal endocervical glands frequently express MUC5AC,[33,34] we believe that focal positivity observed in EMBTs are due most probably to the MUC5AC antibody reacting to Müllerian type mucinous epithelium that does not necessarily have gastric foveolar-type characteristics. In the past, the presence of goblet cells has been emphasized as a characteristic of IMBTs that can be observed in almost all cases[7,9,10] and a number of studies have focused on the expression of intestinal markers such as CDX2 and MUC2 as key immunophenotypes of IMBT.[2,12,35] However, similar to some previous reports,[35,36] CDX2 and MUC2 expression in IMBTs was observed in fewer than half the cases, and their immunoreactivity was often focal in this study. Therefore, we conclude that in general IMBTs are composed essentially of gastrointestinal-type mucinous epithelium, the predominant component of which is gastric- rather than intestinal-type epithelium. This notion coincides with the morphological assessment of IMBTs by us and other researchers who consider that most

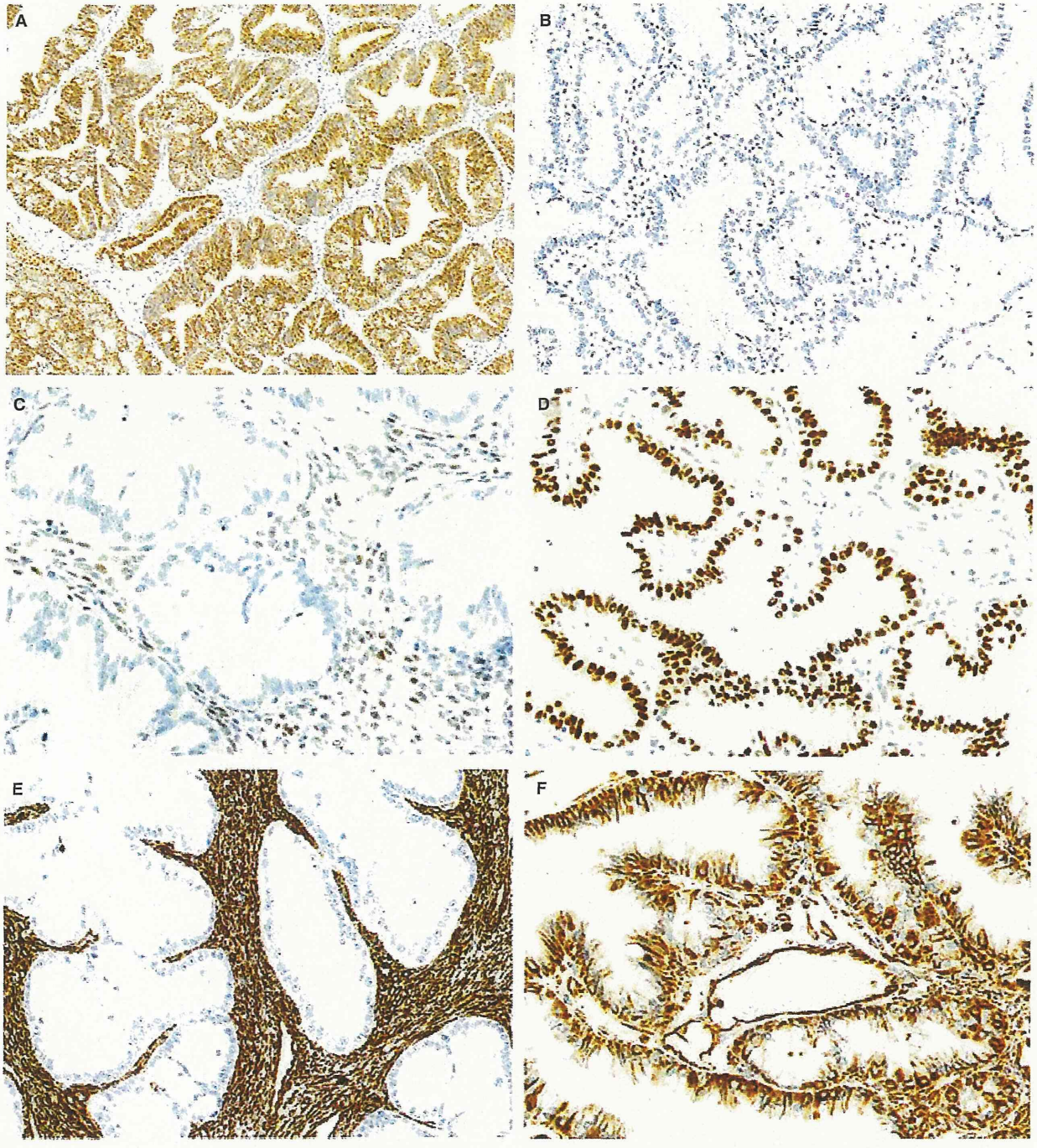

Figure 3. Expression of CK20, ER and vimentin in (A,C,E) intestinal-type mucinous borderline tumour (IMBT) (B,D,F) endocervical-like borderline tumour (EMBT). (A) IMBT showing strong CK20 expression. (B) CK20 is negative in EMBT. (C) ER is usually negative in IMBTs. (D) EMBTs always show diffuse and strong nuclear ER positivity. (E) Vimentin expression is seen only in the stroma of IMBTs. The tumour cells are vimentin-negative. (F) Vimentin expression in an EMBT. Many of the tumour cells show positive immunoreactivity along with stromal cells.

mucinous epithelium in IMBTs resembles foveolar-type gastric epithelium.[2,14] Therefore, we propose abandoning the nomenclature 'intestinal-type mucinous borderline tumour' and replacing it with 'gastrointestinal-type mucinous borderline tumour' to avoid further confusion.

Table 4. Immunophenotype of serous borderline tumours

	CLDN18	MUC1	MUC2	MUC5AC	MUC6	CDX2	CK7	CK20	ER	PgR	CA125	Vimentin
–	22	0	22	21	22	22	0	22	0	1	0	0
1+	0	0	0	1	0	0	0	0	0	1	0	2
2+	0	0	0	0	0	0	0	0	0	0	0	0
3+	0	0	0	0	0	0	1	0	0	3	0	3
4+	0	22	0	0	0	0	21	0	22	17	22	17
Total	0/22 (0%)	22/22 (100%)	0/22 (0%)	1/22 (5%)	0/22 (0%)	0/22 (0%)	22/22 (100%)	0/22 (0%)	22/22 (100%)	21/22 (95%)	22/22 (100%)	22/22 (100%)

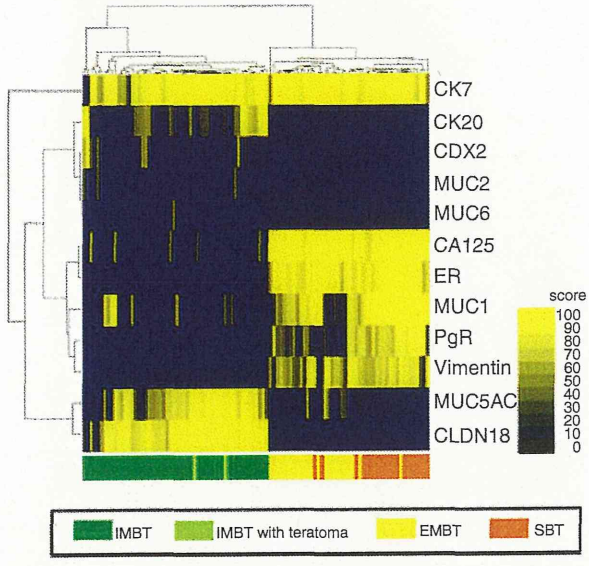

Figure 4. Unsupervised two-way hierarchical clustering based on the protein expression of ovarian borderline tumours. Intestinal-type mucinous borderline tumours (IMBT) were grouped separately from endocervical-like mucinous borderline tumours (EMBT) and serous borderline tumours (SBT). Similarities between the immunoprofiles of EMBTs and SBTs are demonstrated.*

Our immunohistochemical panel highlighted the differences between EMBTs and IMBTs. Similarities between EMBTs and SBTs have been described repeatedly from the morphological and immunohistochemical points of view.[2,3,16] Recent studies have reported that EMBTs share features with low-grade endometrioid tumours (borderline tumours and carcinomas), such as frequent association with endometriosis and frequent loss of ARID1A expression.[8] Currently, it is not clear whether EMBTs are closer to SBTs or low-grade endometrioid tumours. We recognize EMBT as a distinct Müllerian-type tumour that shows a variable degree of mucin production. In fact, our study revealed a Müllerian immunophenotype for EMBTs, including positivity for ER, PgR, CA-125 and vimentin. Furthermore, hierarchical clustering of ovarian borderline tumours (IMBTs, EMBTs and SBTs) according to their protein expression resulted in the grouping of EMBTs and SBTs together in a cluster that was completely separate from the IMBT cluster. Although the number of antibodies applied in this study was limited and there was limitation in terms of assessing intratumoral heterogeneity due to the use of TMAs, the data show clearly that EMBT and IMBT are two

*Figure 4 was corrected on 07/08/2013 after first online publication 06/05/2013. "CLDN18" was incorrectly spelled "CLND18".

distinct neoplasms and that the former is a part of the ovarian Müllerian-type tumour spectrum.

From a diagnostic standpoint, pathologists may occasionally encounter ovarian mucinous tumours that are difficult to classify as either IMBT or EMBT. In such instances, we propose that the best immunohistochemical panel is a combination of CLDN18, CK20, ER and vimentin. IMBTs most frequently show a CLDN18$^+$/CK20$^+$/ER$^-$/vimentin$^-$ pattern, whereas EMBTs are almost always CLDN18$^-$/CK20$^-$/ER$^+$/vimentin$^+$.

In summary, we report overexpression of a gastric marker, CLDN18, in ovarian IMBTs. The distinct nature of IMBTs and EMBTs was elucidated through immunohistochemical analyses using a panel of antibodies including CLDN18. We have also shown that CLDN18 can serve as a good diagnostic marker to distinguish IMBT from EMBT. Taking these results into consideration, we hope to emphasize that IMBTs are essentially 'gastrointestinal-type mucinous borderline tumours' and that EMBTs are 'Müllerian-type mucinous borderline tumours'. With regard to the tumorigenesis of ovarian gastrointestinal-type mucinous tumours, future studies of the origin of gastric-type epithelium in the ovary are warranted.

Acknowledgements

The authors would like to thank Yumiko Nagano for her tremendous technical support. This work was supported by a Grant-in-Aid for Scientific Research (KAKENHI) from the Japan Society for the Promotion of Science.

Conflict of interests

None declared.

References

1. Tavassoli FA, Devilee P, eds. *Pathology and genetics of tumours of the breast and female genital organs*. Lyon: IARC Press, 2003; 124–129.
2. Vang R, Gown AM, Barry TS, Wheeler DT, Ronnett BM. Ovarian atypical proliferative (borderline) mucinous tumors: gastrointestinal and seromucinous (endocervical-like) types are immunophenotypically distinctive. *Int. J. Gynecol. Pathol.* 2006; **25**; 83–89.
3. Yasunaga M, Ohishi Y, Oda Y *et al.* Immunohistochemical characterization of mullerian mucinous borderline tumors: possible histogenetic link with serous borderline tumors and low-grade endometrioid tumors. *Hum. Pathol.* 2009; **40**; 965–974.
4. Nakatsuka S, Wakimoto T, Ozaki K *et al.* Mucinous borderline-like tumor of the gastrointestinal type arising from mature cystic teratoma of the ovary and its immunohistochemical cytokeratin and mucin phenotype. *J. Obstet. Gynaecol. Res.* 2012; **38**; 471–475.
5. Vang R, Gown AM, Barry TS, Wheeler DT, Ronnett BM. Immunohistochemistry for estrogen and progesterone receptors in the distinction of primary and metastatic mucinous tumors in the ovary: an analysis of 124 cases. *Mod. Pathol.* 2006; **19**; 97–105.
6. Shappell HW, Riopel MA, Smith Sehdev AE, Ronnett BM, Kurman RJ. Diagnostic criteria and behavior of ovarian seromucinous (endocervical-type mucinous and mixed cell-type) tumors: atypical proliferative (borderline) tumors, intraepithelial, microinvasive, and invasive carcinomas. *Am. J. Surg. Pathol.* 2002; **26**; 1529–1541.
7. Acs G. Serous and mucinous borderline (low malignant potential) tumors of the ovary. *Am. J. Clin. Pathol.* 2005; **123**(Suppl); S13–S57.
8. Wu CH, Mao TL, Vang R *et al.* Endocervical-type mucinous borderline tumors are related to endometrioid tumors based on mutation and loss of expression of arid1a. *Int. J. Gynecol. Pathol.* 2012; **31**; 297–303.
9. Nomura K, Aizawa S. Clinicopathologic and mucin histochemical analyses of 90 cases of ovarian mucinous borderline tumors of intestinal and Müllerian types. *Pathol. Int.* 1996; **46**; 575–580.
10. Hart WR. Borderline epithelial tumors of the ovary. *Mod. Pathol.* 2005; **18**(Suppl 2); S33–S50.
11. Moriya T, Mikami Y, Sakamoto K *et al.* Endocervical-like mucinous borderline tumors of the ovary: clinicopathological features and electron microscopic findings. *Med. Electron Microsc.* 2003; **36**; 240–246.
12. Vang R, Gown AM, Zhao C *et al.* Ovarian mucinous tumors associated with mature cystic teratomas: morphologic and immunohistochemical analysis identifies a subset of potential teratomatous origin that shares features of lower gastrointestinal tract mucinous tumors more commonly encountered as secondary tumors in the ovary. *Am. J. Surg. Pathol.* 2007; **31**; 854–869.
13. Boman F, Buisine MP, Wacrenier A, Querleu D, Aubert JP, Porchet N. Mucin gene transcripts in benign and borderline mucinous tumours of the ovary: an *in situ* hybridization study. *J. Pathol.* 2001; **193**; 339–344.
14. Ji H, Isacson C, Seidman JD, Kurman RJ, Ronnett BM. Cytokeratins 7 and 20, DPC4, and MUC5AC in the distinction of metastatic mucinous carcinomas in the ovary from primary ovarian mucinous tumors: DPC4 assists in identifying metastatic pancreatic carcinomas. *Int. J. Gynecol. Pathol.* 2002; **21**; 391–400.
15. Rutgers JL, Scully RE. Ovarian mixed-epithelial papillary cystadenomas of borderline malignancy of mullerian type. A clinicopathologic analysis. *Cancer* 1988; **61**; 546–554.
16. Rutgers JL, Scully RE. Ovarian mullerian mucinous papillary cystadenomas of borderline malignancy. A clinicopathologic analysis. *Cancer* 1988; **61**; 340–348.
17. Siriaunkgul S, Robbins KM, McGowan L, Silverberg SG. Ovarian mucinous tumors of low malignant potential: a clinicopathologic study of 54 tumors of intestinal and Müllerian type. *Int. J. Gynecol. Pathol.* 1995; **14**; 198–208.
18. Rodriguez IM, Irving JA, Prat J. Endocervical-like mucinous borderline tumors of the ovary: a clinicopathologic analysis of 31 cases. *Am. J. Surg. Pathol.* 2004; **28**; 1311–1318.
19. Fukunaga M, Ushigome S. Epithelial metaplastic changes in ovarian endometriosis. *Mod. Pathol.* 1998; **11**; 784–788.
20. Mineta K, Yamamoto Y, Yamazaki Y *et al.* Predicted expansion of the claudin multigene family. *FEBS Lett.* 2011; **585**; 606–612.
21. Tsukita S, Furuse M. Pores in the wall: claudins constitute tight junction strands containing aqueous pores. *J. Cell Biol.* 2000; **149**; 13–16.

22. Tamura A, Yamazaki Y, Hayashi D *et al.* Claudin-based paracellular proton barrier in the stomach. *Ann. NY Acad. Sci.* 2012; **1258**; 108–114.
23. Shinozaki A, Ushiku T, Morikawa T *et al.* Epstein–Barr virus-associated gastric carcinoma: a distinct carcinoma of gastric phenotype by claudin expression profiling. *J. Histochem. Cytochem.* 2009; **57**; 775–785.
24. Shinozaki A, Shibahara J, Noda N *et al.* Claudin-18 in biliary neoplasms. Its significance in the classification of intrahepatic cholangiocarcinoma. *Virchows Arch.* 2011; **459**; 73–80.
25. Tanaka M, Shibahara J, Fukushima N *et al.* Claudin-18 is an early-stage marker of pancreatic carcinogenesis. *J. Histochem. Cytochem.* 2011; **59**; 942–952.
26. Matsuda M, Sentani K, Noguchi T *et al.* Immunohistochemical analysis of colorectal cancer with gastric phenotype: claudin-18 is associated with poor prognosis. *Pathol. Int.* 2010; **60**; 673–680.
27. Sahin U, Koslowski M, Dhaene K *et al.* Claudin-18 splice variant 2 is a pan-cancer target suitable for therapeutic antibody development. *Clin. Cancer Res.* 2008; **14**; 7624–7634.
28. Hewitt KJ, Agarwal R, Morin PJ. The claudin gene family: expression in normal and neoplastic tissues. *BMC Cancer* 2006; **6**; 186.
29. Sanada Y, Oue N, Mitani Y, Yoshida K, Nakayama H, Yasui W. Down-regulation of the claudin-18 gene, identified through serial analysis of gene expression data analysis, in gastric cancer with an intestinal phenotype. *J. Pathol.* 2006; **208**; 633–642.
30. Ricardo S, Gerhard R, Cameselle-Teijeiro JF, Schmitt F, Paredes J. Claudin expression in breast cancer: high or low, what to expect? *Histol. Histopathol.* 2012; **27**; 1283–1295.
31. Sentani K, Oue N, Tashiro T *et al.* Immunohistochemical staining of Reg IV and claudin-18 is useful in the diagnosis of gastrointestinal signet ring cell carcinoma. *Am. J. Surg. Pathol.* 2008; **32**; 1182–1189.
32. Hayashi D, Tamura A, Tanaka H *et al.* Deficiency of claudin-18 causes paracellular h+ leakage, up-regulation of interleukin-1β, and atrophic gastritis in mice. *Gastroenterology* 2012; **142**; 292–304.
33. Baker AC, Eltoum I, Curry RO *et al.* Mucinous expression in benign and neoplastic glandular lesions of the uterine cervix. *Arch. Pathol. Lab. Med.* 2006; **130**; 1510–1515.
34. Ota H, Harada O, Uehara T, Hayama M, Ishii K. Aberrant expression of TFF1, TFF2, and PDX1 and their diagnostic value in lobular endocervical glandular hyperplasia. *Am. J. Clin. Pathol.* 2011; **135**; 253–261.
35. Hirabayashi K, Yasuda M, Kajiwara H *et al.* Alterations in mucin expression in ovarian mucinous tumors: immunohistochemical analysis of mUC2, MUC5AC, MUC6, and CD10 expression. *Acta Histochem. Cytochem.* 2008; **41**; 15–21.
36. Vang R, Gown AM, Wu LS *et al.* Immunohistochemical expression of CDX2 in primary ovarian mucinous tumors and metastatic mucinous carcinomas involving the ovary: comparison with CK20 and correlation with coordinate expression of CK7. *Mod. Pathol.* 2006; **19**; 1421–1428.

OPEN ACCESS Freely available online

PLOS ONE

A Novel Interaction between hScrib and PP1γ Downregulates ERK Signaling and Suppresses Oncogene-Induced Cell Transformation

Kazunori Nagasaka[1], Takayuki Seiki[1], Aki Yamashita[1], Paola Massimi[2], Vanitha Krishna Subbaiah[2], Miranda Thomas[2], Christian Kranjec[2], Kei Kawana[1], Shunsuke Nakagawa[3], Tetsu Yano[1], Yuji Taketani[1], Tomoyuki Fujii[1], Shiro Kozuma[1], Lawrence Banks[2]*

1 Department of Obstetrics and Gynecology, Faculty of Medicine, The University of Tokyo, Tokyo, Japan, **2** International Centre for Genetic Engineering and Biotechnology, Area Science Park, Trieste, Italy, **3** Department of Obstetrics and Gynecology, The Teikyo University School of Medicine, Tokyo, Japan

Abstract

Previous studies have shown that the cell polarity regulator hScrib interacts with, and consequently controls, the ERK signaling pathway. This interaction occurs through two well-conserved Kinase Interacting Motifs, which allow hScrib to bind ERK1 directly, resulting in a reduction in the levels of phospho-ERK. This suggests that hScrib might recruit a phosphatase to regulate this signaling pathway. Using a proteomic approach we now show that Protein Phosphatase 1γ (PP1γ) is a major interacting partner of hScrib. This interaction is direct and occurs through a conserved PP1γ interaction motif on the hScrib protein, and this interaction appears to be required for hScrib's ability to downregulate ERK phosphorylation. In addition, hScrib also controls the pattern of PP1γ localization, where loss of hScrib enhances the nuclear translocation of PP1γ. Furthermore, we also show that the ability of hScrib to interact with PP1γ is important for the ability of hScrib to suppress oncogene-induced transformation of primary rodent cells. Taken together, these results demonstrate that hScrib acts as a scaffold to integrate the control of the PP1γ and ERK signaling pathways and explains how disruption of hScrib localisation can contribute towards the development of human malignancy.

Citation: Nagasaka K, Seiki T, Yamashita A, Massimi P, Subbaiah VK, et al. (2013) A Novel Interaction between hScrib and PP1γ Downregulates ERK Signaling and Suppresses Oncogene-Induced Cell Transformation. PLoS ONE 8(1): e53752. doi:10.1371/journal.pone.0053752

Editor: Cara Gottardi, Northwestern University Feinberg School of Medicine, United States of America

Received January 29, 2012; **Accepted** December 4, 2012; **Published** January 24, 2013

Funding: This work was supported by research grants from the Okinaka Memorial Institute for Medical Research (to K.N.) and by a Grant-in-Aid for Scientific Research (no. 24592506, to K.N.) from the Ministry of Education, Science and Culture, Japan, and by research grants from the Associazione Italiana per la Ricerca sul Cancro and the Wellcome Trust (to L.B.). The funders had no role in study design, data collection and analysis, decision to publish, or preparation of the manuscript.

Competing Interests: The authors have declared that no competing interests exist.

* E-mail: banks@icgeb.org

Introduction

The control of cell polarity and the maintenance of tissue architecture are intimately related and are, in part, controlled by a tri-partite macromolecular signaling complex consisting of the Scrib complex, the Par complex and the Crumbs complex [1,2]. Through a series of antagonistic interactions the components of these three complexes control a variety of downstream signaling pathways that, in turn, directly contribute to the regulation of cell polarity and cell proliferation [3]. It is now clear that the loss of control of these pathways is a common event during the development of diverse human malignancies [1,4–7]. These defects are particularly evident at the later stages of malignant progression, and a variety of studies in both Drosophila and transgenic mice have provided additional supporting evidence of tumour suppressor activity for the various components of these signaling complexes [8–11].

The hScrib complex consists of three proteins, hScrib, hDlg1 and Hugl-1/2. In *Drosophila*, loss of either Scrib or Dlg produces imaginal disc overgrowth with invasive characteristics [8] [12], phenotypes that can be functionally complemented by the mammalian equivalents [13–15]. More recently Scrib has been implicated in the control of the JNK and ERK signaling cascades, and loss of hScrib appears to enhance the effects of the Ras and Myc oncogenes, and can contribute to mammary tumour development [16–21]. Recent studies have also demonstrated that hScrib can interact directly with ERK, and control both ERK activation and its nuclear translocation [19]. However, the physical interaction between ERK and hScrib is not sufficient to explain the inactivation of ERK, since high levels of hScrib appear capable of directly reducing the levels of ERK phosphorylation [19]. Since hScrib has no known phosphatase activity itself, it therefore seemed possible that a protein phosphatase might be recruited by hScrib to fully inactivate the ERK signaling pathway.

Control of ERK activation reflects an exquisite balance between the activities of the activating kinases and the de-activating protein phosphatases. Activated ERK can translocate to the nucleus, where it activates several transcription factors and also phosphorylates cytoplasmic and nuclear kinases [22–24]. Since phosphorylation of both the threonine and tyrosine residues of ERK is required for its activation, dephosphorylation of either is sufficient for its inactivation [25]. There are several reports demonstrating that dephosphorylation of active ERK can be achieved by tyrosine-specific phosphatases, by serine/threonine-specific phos-

phatases or by dual specificity (threonine/tyrosine) protein phosphatases [26–29]. One of the important negative regulators of the ERK signaling pathway is PP2A, a member of the PPP family of protein serine/threonine phosphatases which also includes PP1 [30,31]. However, PP2A is thought to exert its activity mainly upon other activating kinases within the cascade, rather than upon ERK itself [32–34]. In addition, recent studies have also shown that hScrib can directly regulate the Akt signaling cascade by recruitment of the protein phosphatase PHLPP1 to the plasma membrane, thereby resulting in de-phosphorylation of Akt [35]. Here, we have used a proteomic approach to extend our investigations into the regulation of the ERK signaling cascade by hScrib. We now show that hScrib interacts with PP1γ, and that this association correlates with the ability of hScrib to downregulate ERK activation. We also provide compelling evidence that hScrib directly contributes to the regulation of PP1γ function by controlling its translocation between the cytoplasm and the nucleus. Thus, loss of hScrib expression results in both ERK activation and aberrant nuclear translocation of PP1γ.

Materials and Methods

Cells and treatments

HEK293 (human embryonic kidney cells) and HaCaT (Human keratinocytes) were obtained from ATCC [36,37]. HEK293, HaCaT and Baby Rat Kidney (BRK) cells were cultured in Dulbecco's modified Eagle's medium (DMEM) supplemented with 10% fetal bovine serum, penicillin-streptomycin (100 U/mL) and glutamine (300 μg/mL) in a humidified 5%CO_2 incubator. Transfection was carried out using calcium phosphate precipitation as described previously [37] or using Lipofectamine 2000 (Invitrogen) according to the manufacturer's protocol. The depleted Scribble cell lines were generated as described previously [19]. Cell transformation assays were done using BRK cells obtained from 9 day old Wistar rats with a combination of HPV-16 E7 and EJ-ras, plus the appropriate hScrib and PP1γ expression plasmids. Cells were placed under G418 selection for three weeks, and then fixed and stained.

Plasmids

The wild type pCDNA3-HA-PP1γ was the kind gift of Dr. Wilhelm Krek (Swiss Federal Institute of Technology (ETH) Zurich). The wild type HA-tagged pcDNA hScrib expression plasmid and the truncated mutant pGEX hScrib PDZ1-C, PDZ1-4, S1445A, S1445D, and CT expression plasmids have been described previously [19]. The L1266Y1268→AA mutation (KADA) to doubly change the Leucine (L) and Tyrosine (Y) residues to Alanine (A) in hScrib was done using the QuikChange site-directed mutagenesis kit from Stratagene Cloning Systems (Celbio) according to the manufacturer's instruction. The mutants were confirmed by DNA sequencing. See Figure S1 for a detailed description of the location of the different hScrib mutations.

Antibodies

The following commercial antibodies were used at the dilution indicated: anti-hScrib goat polyclonal antibody (Santa Cruz, WB 1:1000), anti-PP1γ goat polyclonal antibody (Santa Cruz, WB 1:1000), anti-PP1γ sheep polyclonal antibody (Abcam, WB 1:1000), anti-p44/42 MAPK (Erk1/2) antibody (Cell Signaling Technology, WB 1:1000), anti-phospho p44/42 MAPK (Erk1/2) (Thr202/Tyr204) antibody (Cell Signaling Technology, WB 1:1000), anti-HA monoclonal antibody 12CA5 (Roche, WB 1:500), anti-γ-tubulin monoclonal antibody (Sigma, WB 1:5000), anti-p84 mouse monoclonal antibody (Abcam, WB 1:1000), anti-E-Cadherin rabbit polyclonal antibody (Santa Cruz, WB 1:500), anti-α-tubulin mouse monoclonal antibody (Abcam, WB 1:1000).

Immunofluorescence and Microscopy

For immunofluorescence cells were grown on glass coverslips and fixed in 3.7% paraformaldehyde in PBS for 20 mins at room temperature. After washing in PBS the cells were permeabilised in PBS/0.1% Triton for 5 mins, washed extensively in PBS and then incubated with primary antibody diluted in PBS for 1 hour followed by the appropriately conjugated secondary antibodies. Secondary antibodies conjugated to Alexa Fluor 488 or 548 were obtained from Invitrogen. The cells were then washed several times in water and mounted on glass slides. Cells were visualized by using a Zeiss Axiovert 100 M microscope attached to a LSM 510 confocal unit.

siRNA transfection

HEK293 cells were seeded on 6 cm dishes and transfected using Lipofectamine 2000 (Invitrogen) with control siRNA against Luciferase (siLuc), or siRNA against hScrib and PP1γ sequences (Dharmancon). 48 hours post-transfection cells were harvested and total cells extracts or cell fractionated extracts were then analysed by western blotting.

Fusion protein purification and in vitro binding assays

GST-tagged fusion proteins were expressed and purified as described previously [19]. Proteins were translated in vitro using the Promega TNT kit and radiolabelled with (^{35}S) cysteine or (^{35}S) methionine (Perkin Elmer). Equal amounts of in vitro-translated proteins were added to GST fusion proteins bound to glutathione agarose (Sigma) and incubated for 1 hour at 4°C. After extensive washing with PBS containing 0.25% NP-40, or as otherwise indicated, the bound proteins were analysed by SDS-PAGE and autoradiography.

In vitro phosphorylation

Purified GST fusion proteins were incubated with commercially purified ERK1 (Cell Signaling Technology) or PKA (Promega) for 20 mins at 30°C in phosphorylation buffer (0.25 M Tris pH7.5, 1 M $MgCl_2$, 3 M NaCl, 0.3 mM aprotinin, 1 mM Pepstatin) or using the kinase buffer supplied by New England Biolabs supplemented with 56 nM (^{32}P) γ-ATP (Perkin Elmer) and 10 mM ATP following the manufacturer's instruction. After extensive washing, the phosphorylated proteins were monitored by SDS-PAGE and autoradiography.

Mass spectrometry analysis

HEK293 cells were transfected with HA-tagged Scrib and after 24 hours the cells were extracted in mass spectrometry lysis buffer (50 mM Hepes pH 7.4, 150 mM NaCl, 50 mM NaF, 1 mM EDTA, 0.25% NP40) and extracts incubated with anti-HA beads (Sigma) for 2–3 hours on a rotating wheel at 4°C. The beads were then extensively washed with PBS, dried and the immunoprecipitated proteins were subjected to proteomic analysis as described previously [38].

Subcellular Fractionation assays

Differential extraction of HEK 293 cells to obtain cytoplasmic, membrane, cytoskeleton, and nuclear fractions was performed using the Calbiochem ProteoExtract Fractionation Kit according to the manufacturer's instructions. To inhibit phosphatase activity during the preparation of cell lysates, phosphatase inhibitors

A

log (e)+	#	total	HA-Scribble
-1189.3	91	200	SCRIB, scribble
-327.5	29	37	VIM, vimentin
-73.2	6	10	NPM1P21, nucleophosmin
-60.5	6	6	PPP1CC, protein phosphatase 1, catalytic subunit, gamma isoform
-59.6	6	6	NCL, nucleolin

ADLDKLNIDS IIQR [15]Ilev
LFEYGGFPPE SNYLFLGDYV DR [96]gkqs
IKYPENFFLL R [122]gnhe
YPENFFLLR [122]gnhe
AHQVVEDGYE FFAK [260]rqlv
KKPNATRPVT PPR [314]gmit

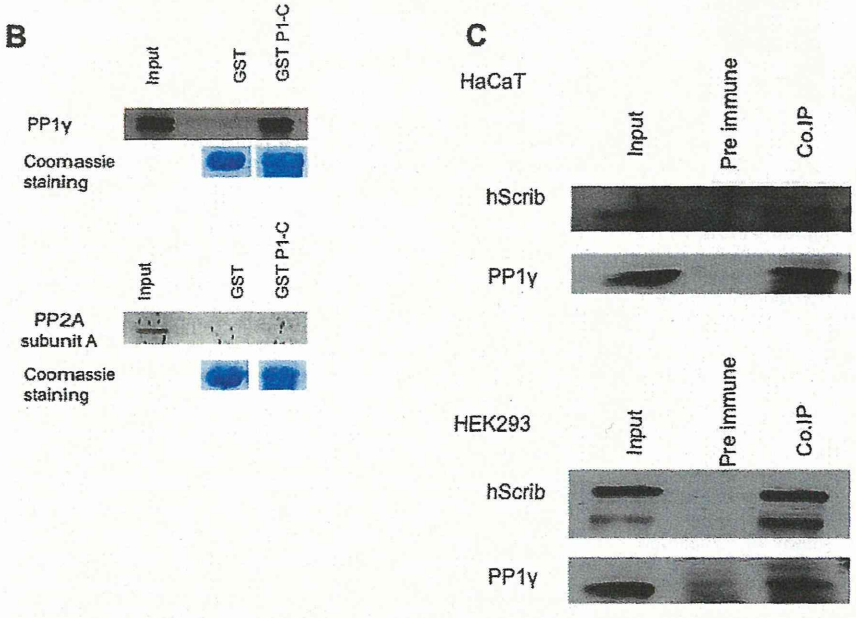

Figure 1. Interaction between hScrib and PP1γ in vivo. A) Results from the mass spectroscopy analysis of hScrib containing immunoprecipitates identified 6 peptides (indicated) corresponding to PP1γ. B) In vitro translated PP1γ (upper panels) and PP2A subunit A (lower panels) were incubated for 1 hour at 4°C with purified GST-hScribP1-C or GST alone immobilized on Glutathione agarose. After extensive washing, the bound proteins were analysed by SDS–PAGE and autoradiography which are shown in each of the upper panels. The gels were rehydrated and stained with Coomassie to show equal levels of GST loading in the respective lower panels. C) Endogenous PP1γ was immunoprecipitated from HaCaT (upper panels) and HEK 293 cells (lower panels), with pre-immune antibody used as control. The immunoprecipitated proteins were then analysed by western blotting using anti-hScrib and anti-PP1γ antibodies.
doi:10.1371/journal.pone.0053752.g001

(1 mM Na_3VO_4, 1 mM β-Glycerophosphate, 2.5 mM Sodium Pyrophosphate, 1 mM Sodium Fluoride) were also included.

Immunoprecipitation and Western blotting

Total cellular extracts were prepared by directly lysing cells from dishes in SDS lysis buffer. Alternatively cells were lysed in either E1A buffer (25 mM HEPES pH 7.0, 0.1% NP-40, 150 mM NaCl, plus protease inhibitor cocktail; Calbiochem) or RIPA buffer (50 mM Tris HCl pH 7.4, 1% NP-40, 150 mM NaCl, 1 mM EDTA, plus protease inhibitor cocktail; Calbiochem) and the cell extracts were analysed by SDS-PAGE and western blotting. For immunoprecipitations, total cell lysates were transferred into a tube of equilibrated EZview Red Anti-HA Affinity Gel beads (Sigma), and incubated for 2 hours at 4°C. Immunoprecipitates were extensively washed four times in lysis buffer and solubilised in SDS-PAGE sample buffer. For western blotting, 0.45 μm nitrocellulose membrane (Schleicher and Schuell) was used and membranes were blocked for 1 hour at 37°C in 10% milk/PBS followed by incubation with the appropriate primary antibody diluted in 10% milk/0.5% Tween 20 for 1 hour. After

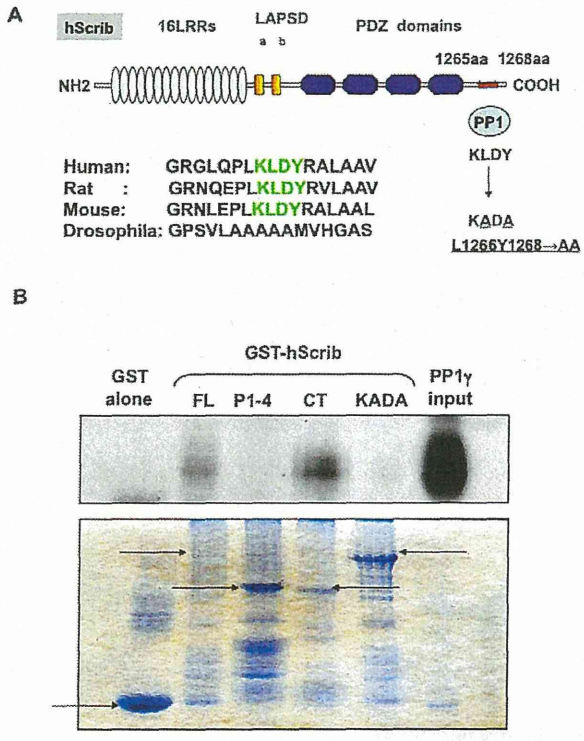

Figure 2. hScrib contains a consensus PP1-binding motif. A) The schematic shows the arrangement of the functional domains on the hScrib protein, highlighting the LRR, LAPSD and PDZ domains. The putative PP1-binding site, the RVXF (the consensus sequence is K/R/H/N/S V/I/L X F/W/Y) motif is also shown, where X is any amino acid. The hScrib mutant in which the PP1-binding site KLDY was mutated to KADA in order to disrupt the interaction with PP1 is shown. A comparison sequence alignment of the region of hScrib containing the PP1-binding motif indicating its absence in Drosophila also shown. B) In vitro translated and radiolabeled PP1γ was incubated with purified full length GST-hScrib fusion protein (FL), GST-hScrib PDZ1-4 (P1-4), GST-hScrib CT (CT), GST-hScrib L1266Y1268→AA (KADA) and GST alone as a control. After extensive washing the bound PP1γ was ascertained by SDS PAGE and autoradiography. The upper panel shows the autoradiograph, with the input of PP1γ also shown for comparison. The lower panel shows the Coomassie stain of the gel showing the levels of GST fusion protein loading, with the arrows indicating the relevant full length fusion proteins.
doi:10.1371/journal.pone.0053752.g002

several washings with PBS 0.5% Tween 20, secondary antibodies conjugated with HRP (DAKO) in 10% milk/0.5% Tween 20 were incubated for 1 hour. Blots were developed using Amersham ECL reagents according to the manufacturer's instructions.

Results

PP1γ is a direct binding partner of hScrib

Based on our previous studies we reasoned that down-regulation of ERK phosphorylation by hScrib might involve the recruitment of a protein phosphatase [19]. To investigate this possibility we performed proteomic analyses to identify additional interacting partners of hScrib. HEK293 cells were transfected with an HA-tagged hScrib expression plasmid and after 24 hours the cells were extracted, and hScrib–bound protein complexes were immunoprecipitated with anti-HA agarose beads and then subjected to mass spectroscopy analysis. Several previously reported interacting partners were identified, including vimentin. However, of the novel interacting partners, the most prominent phosphatase identified was the catalytic subunit of PP1γ (Figure 1A), a major eukaryotic serine/threonine protein phosphatase. To investigate whether hScrib can interact with PP1γ, an in vitro pull-down assay was performed using purified GST-hScrib P1-C fusion protein and in vitro translated radiolabeled PP1γ. For comparison a similar assay was also done using in vitro translated radiolabeled protein phosphatase 2A (PP2A). After extensive washing the bound PP1γ and PP2A were detected by SDS PAGE and autoradiography, and the results in Figure 1B demonstrate strong interaction between hScrib and PP1γ. In contrast, no interaction was observed between hScrib and PP2A, confirming the specificity of the association between hScrib and PP1γ. To determine whether endogenous hScrib and PP1γ could exist in a complex in vivo, immunoprecipitations were performed on cell extracts from HEK293 and HaCaT epithelial cells using anti-PP1γ antibody. Co-immunoprecipitated hScrib was then detected by western blotting, and the results in Figure 1C show a significant degree of co-immunoprecipitation of hScrib with PP1γ in both cell lines. Taken together, these results demonstrate that hScrib and PP1γ can exist as a complex in vivo.

hScrib interacts with PP1γ through a conserved RVxF motif

The PP1 holoenzyme is composed of a catalytic subunit and several regulatory subunits, which target the catalytic subunit to specific subcellular locations. The RVxF motif is a short conserved PP1-binding motif initially identified in previous studies showing that these residues can block the interaction of regulatory subunits with the PP1 catalytic subunit [39]. As shown in Figure 2A, analysis of the hScrib sequence reveals the presence of a putative PP1 binding motif, KLDY (the consensus sequence is: {K/R/H/N}.{S/V/I/L}.X.{ F/W/Y}) [40,41] spanning residues 1265–1268. This sequence is also highly conserved in mammalian Scrib proteins, but is absent in Drosphila. Based on previous studies, mutation of the L and Y residues would be expected to severely perturb the interaction with PP1 [39–42]. To investigate whether this KLDY motif is responsible for the capacity of hScrib to bind to PP1γ, a panel of GST-hScrib fusion proteins consisting of the full length (FL), two truncated proteins encompassing PDZ domains 1–4 (P1-4) and the carboxy terminal third of hScrib (CT), plus a full length hScrib with the KLDY/KADA mutation, were used in pull-down assays with in vitro translated radiolabeled PP1γ. The levels of bound PP1γ were then assessed by SDS PAGE and autoradiography and, as can be seen from Figure 2B, PP1γ binds to the carboxy terminal region of hScrib which contains the predicted PP1 binding motif. Furthermore the KLDY/KADA mutation significantly decreases the capacity of PP1γ to interact with hScrib, confirming that the major site of interaction is through the KLDY consensus motif.

hScrib and ERK are substrates of PP1γ

We have previously shown that hScrib is a substrate for both PKA and ERK. Furthermore, hScrib can downregulate ERK activation through a direct protein-protein interaction [19], although the precise mechanism by which hScrib can achieve this is still unknown. We therefore wanted to determine whether phosphorylation of hScrib by either PKA or ERK1 could influence the ability of hScrib to interact with PP1γ and, furthermore, whether hScrib itself was a substrate of PP1γ. To do this, purified GST-hScrib fusion protein was subject to phosphorylation by either PKA or ERK1 in the presence of non-radiolabeled ATP, and after extensive washing binding assays

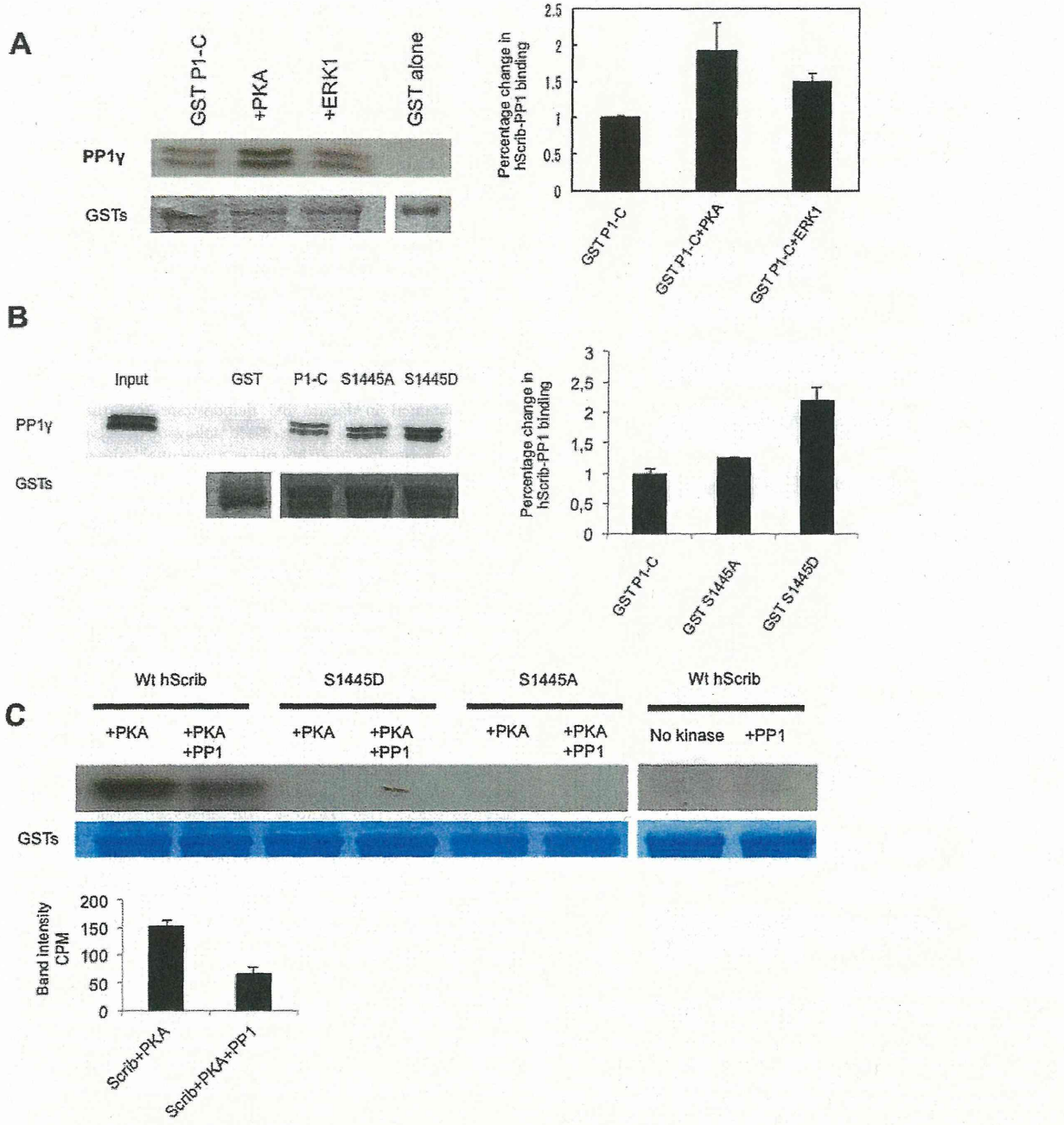

Figure 3. hScrib is a substrate of PP1γ. A) Purified GST-hScrib fusion protein was in vitro phosphorylated with purified PKA or ERK1 as described previously (19) and then incubated with PP1γ for 20 mins at 30°C. Bound PP1γwas detected by western blotting with anti PP1γ antibody. The lower panel shows the ponceau stain of the nitrocellulose, and the upper right panel shows the quantitations from three independent experiments. Note that hScrib phosphorylated by PKA exhibits increased association with PP1γ. B) Purified PP1γ was incubated with purified full length wild type GST-hScrib fusion protein (P1-C), the mutants S1445A, S1445D or GST alone as a control. After extensive washing the bound PP1γ was ascertained by western blotting. The upper panel shows the result of the western blot, with the 20% input of PP1γ also shown for comparison. The lower panel shows the ponceau stain of the nitrocellulose. The histogram shows the quantitation from three independent experiments. C) Purified GST-hScrib wild type and PKA phospho-site mutants of hScrib were in vitro phosphorylated with purified PKA in the presence of radiolabeled ATP as described previously (19) and incubated with PP1γ for 20 mins at 30°C. The remaining level of phosphorylated hScrib was then determined following SDS PAGE and autoradiography. The two right-hand lanes show lack of phosphorylation of hScrib in the absence of PKA, whilst the lower panels show the Coomassie stain of the gel demonstrating equal levels of the GST-hScrib fusion protein throughout. The quantitation of hScrib phosphorylation from three independent experiments is also shown.
doi:10.1371/journal.pone.0053752.g003

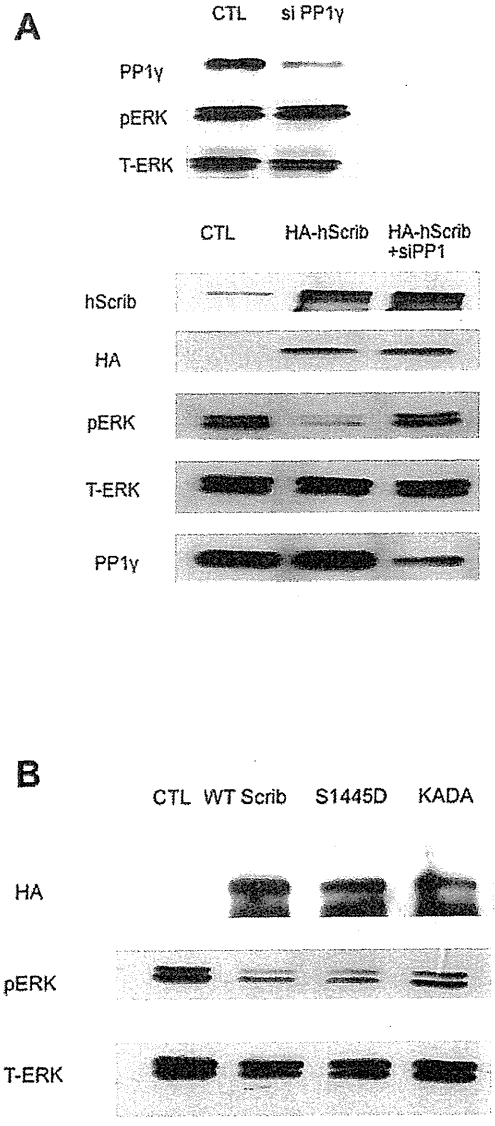

Figure 4. PP1γ is required for hScrib-induced de-phosphorylation of ERK. A) HEK 293 cells were transfected with PP1γ si RNA or si Luc RNA as control (CTL) and after 24 hours were then transfected with a plasmid expressing HA-tagged hScrib. After a further 24 hours the cells were extracted and levels of phospho and total ERK determined by western blot analysis. The upper three panels shows the changes in the ERK profiles when cells were transfected with siRNA PP1γ alone, whilst the lower set of five panels show the effects in the presence of ectopically expressed hScrib. B) HEK 293 cells were transfected with HA-tagged wild type hScrib, or the S1445D and KADA mutants. Total cell extracts were then made after 48 hours and the hScrib, phospho-ERK and total ERK were detected by western blotting.
doi:10.1371/journal.pone.0053752.g004

were performed using commercially purified PP1γ. The bound protein was then detected by western blotting using anti-PP1γ antibodies. The results in Figure 3A demonstrate a number of important features. In the absence of phosphorylation there is a strong interaction between hScrib and the purified PP1γ, demonstrating that the interaction between hScrib and PP1γ is indeed direct. However, there is also a clear increase in the association between hScrib and PP1γ when hScrib is phosphorylated by PKA, but not when it is phosphorylated by ERK1. We had previously shown that the major PKA phosphorylation site on hScrib was S1445 [19]. Therefore, to further confirm that phosphorylation of hScrib by PKA at S1445 can influence its capacity to interact with PP1γ, we repeated the pull down assays using the phospho-mimic mutation of hScrib, S1445D. As can be seen from Figure 3B, the S1445D mutant exhibits a significantly increased capacity to interact with PP1γ, which is similar to that seen following phosphorylation by PKA. These results demonstrate that phosphorylation of hScrib by PKA at S1445 can indeed increase the ability of hScrib to directly interact with PP1γ.

We then analysed whether hScrib was a potential substrate of PP1γ. Purified GST-hScrib fusion protein was subjected to in vitro phosphorylation with purified PKA and radiolabeled ATP. After extensive washing the radiolabeled hScrib fusion protein was incubated with purified PP1γ, and the amount of phosphorylated protein determined by SDS PAGE and autoradiography. The results obtained in Figure 3C demonstrate that the level of phosphorylated hScrib is decreased following incubation with PP1γ, demonstrating that hScrib is a potential substrate of the phosphatase and, furthermore, that hScrib can directly recruit active PP1γ. Also shown are the non-phosphorylatable mutants of hScrib, confirming the specificity of the phosphorylation reaction.

We then proceeded to determine whether the interaction of hScrib with PP1γ might be involved in the capacity of hScrib to downregulate ERK activation. Cells were transfected with control siRNA against luciferase or against PP1γ, and after 24 hours the cells were then transfected with an hScrib expression plasmid. After a further 24 hours the cells were extracted and the levels of activated phospho-ERK analysed by western blotting. The results obtained are shown in Figure 4A. As can be seen, in the absence of hScrib, siRNA PP1γ has minimal effect on the levels of phospho-ERK (Figure 4A upper three panels). In contrast, overexpression of hScrib significantly reduces the levels of phospho-ERK (Figure 4A lower five panels), and this is in agreement with previous studies [19]. However, the ability of hScrib to down-regulate the levels of phospho-ERK is largely abolished following treatment with siRNA PP1γ, suggesting that this activity of hScrib is in part PP1γ-dependent. To further investigate this, we repeated the assay using the PKA phospho-mimic mutant (S1445D) and the non-PP1γ binding mutant (KADA) of hScrib. After 24 hours the levels of phospho-ERK were analysed by western blotting and the results obtained are shown in Figure 4B. As can be seen the wild type and S1445D mutant of hScrib both strongly inhibit the levels of phospho-ERK, whilst the non-PP1γ binding mutant of hScrib is decreased in this activity. Taken together these results demonstrate that the ability of hScrib to interact with PP1γ correlates with its ability to down-regulate the levels of phospho-ERK.

Loss of hScrib enhances PP1γ nuclear localization

Having found that PP1γ plays a role in hScrib regulation of ERK signaling, we were next interested in determining whether hScrib could also potentially affect PP1γ localisation. Therefore, we first analysed the pattern of PP1γ expression in human keratinocytes after stably silencing hScrib expression in these cells. The distribution of PP1γ in control and shScrib HaCaT cells were analysed by immunofluorescence. The results in Figure 5A and Figure 5B, show that most of the PP1γ localises in the nucleus, although some also co-localises with hScrib at the plasma membrane and within the cytoplasm. More importantly, however, upon loss of hScrib expression there is a significant increase in the amount of nuclear PP1γ, with a corresponding decrease in the cytoplasmic pool. In order to verify these results we also performed

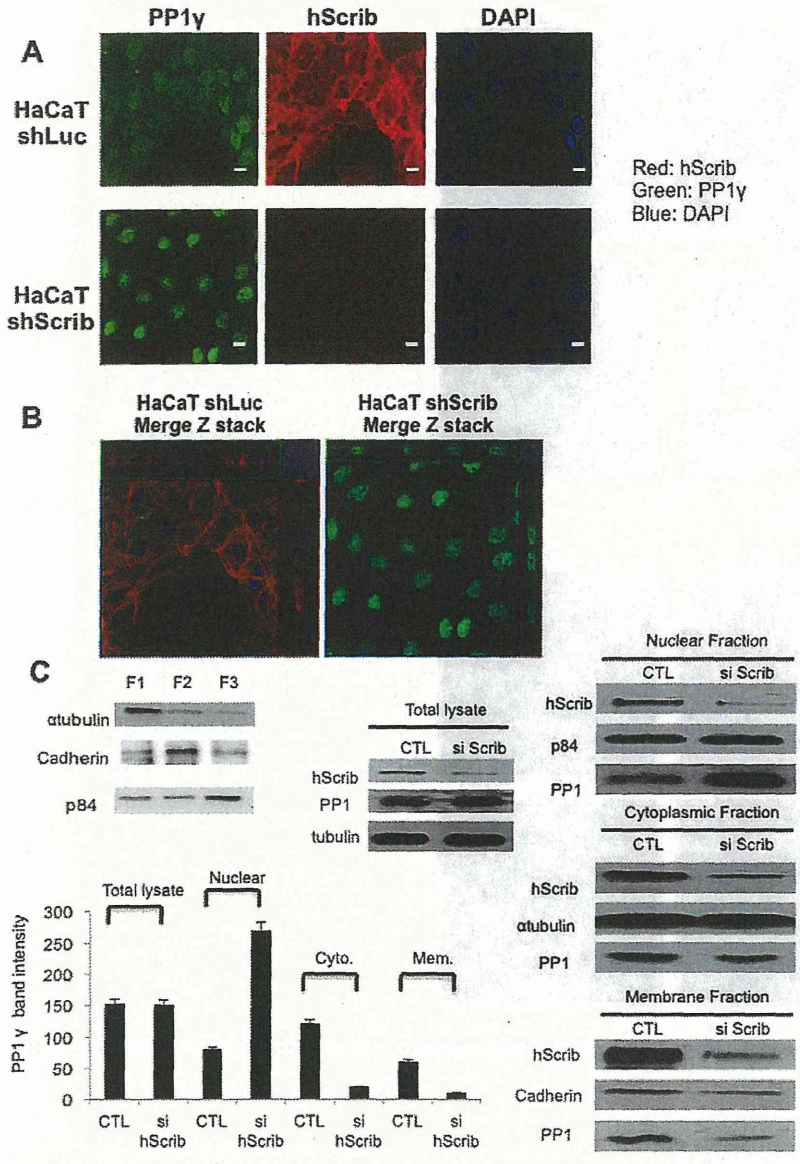

Figure 5. hScrib regulates PP1γ nuclear localization. A) Immunofluorescence analysis of hScrib and PP1γ expression in sh-Luc control HaCaT cells and sh-hScrib knockdown cells. The cells were grown on coverslips and then fixed and double-stained with the anti-hScrib antibody and the anti-PP1γ antibody. Note the significant increase in the levels of nuclear PP1γ in the absence of hScrib expression. B) Z-reconstruction (x-z direction) of a z-stack (15 planes, z-distance 0.2 μm), showing sh-hScrib knockdown cells have enhanced PP1γ localisation into the nucleus. C) HEK 293 cells were transfected with hScrib siRNA and si Luc RNA as control. Cells were either extracted in SDS PAGE sample buffer (Total lysate) or were fractionated into cytoplasmic (F1), membrane (F2) and nuclear (F3) pools (the example shows the integrity of a typical extraction procedure) and then PP1γ was detected by western blotting. p84 was used as a loading control for the nuclear fraction, cadherin was used as a loading control for the membrane fraction and α-tubulin was used as the loading control for the cytoplasmic fraction and total cell extracts. Note the relative increase in nuclear PP1γ following hScrib knockdown but no overall change in total PP1γ levels.
doi:10.1371/journal.pone.0053752.g005

a series of transient siRNA experiments, where hScrib levels were ablated in 293 cells, and the levels of PP1γ, both in total cell extracts or in the respective cellular fractions (Fig. 5C), were analysed by western blotting. As can be seen, loss of hScrib resulted in decreases in the cytoplasmic and membrane pools of PP1γ, but a corresponding increase in the amounts of the nuclear form of the protein.

To investigate the pattern of pERK expression following hScrib depletion we repeated the immunofluorescence assays staining for hScrib, PP1γ and pERK. The results obtained are shown in Figure 6. As can be seen, under conditions of hScrib depletion there is a marked increase in the levels of both nuclear and cytoplasmic pERK, consistent with previous observations [19]. This is also accompanied by an increase in the levels of nuclear PP1γ.

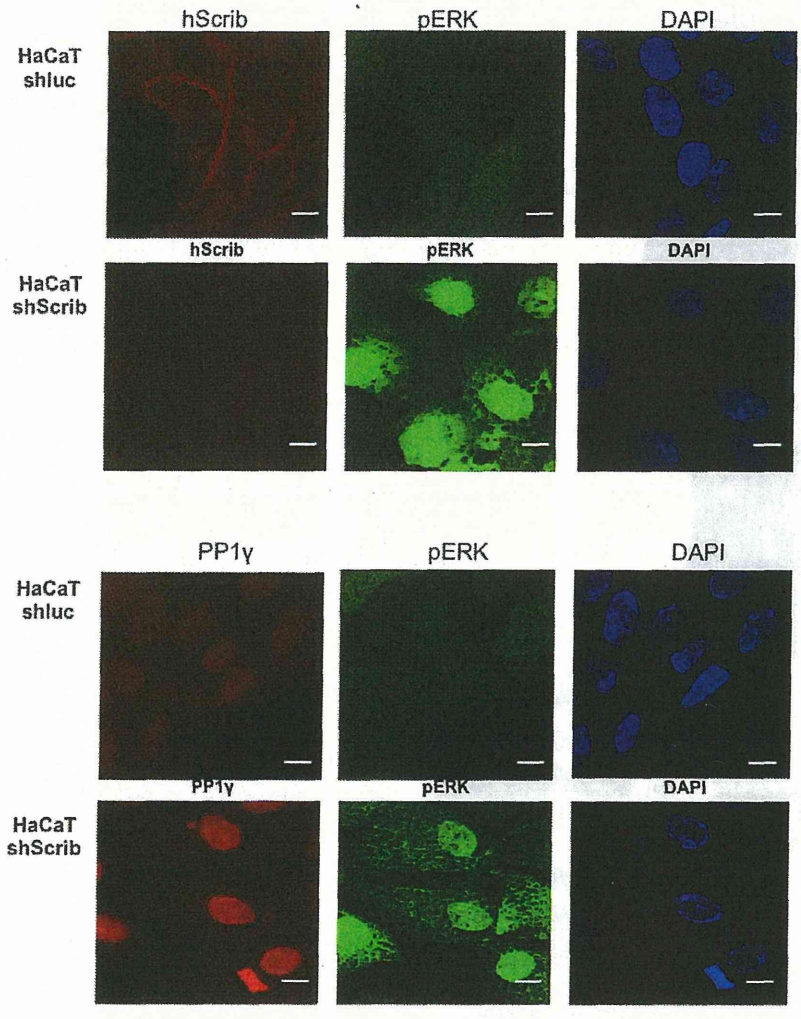

Figure 6. Loss of hScrib results in enhanced nuclear accumulation of both PP1γ and pERK. Control and shScrib HaCaT cells were stained for hScrib, phospho-ERK and PP1γ as indicated.
doi:10.1371/journal.pone.0053752.g006

hScrib tumour suppressor activity requires an intact PP1γ binding motif

We have previously shown that hScrib can suppress cell transformation induced by EJ-ras and Human Papillomavirus (HPV)-16 E7 [19]. To determine whether the interaction between hScrib and PP1γ was physiologically relevant in this context, primary BRK cells were transfected with HPV-16 E7 plus EJ-ras in the presence or absence of the hScrib wild type and KLDY/KADA mutant hScrib expressing plasmids, with or without the PP1γ expression plasmid. After 3 weeks the cells were fixed and stained and the numbers of colonies counted. As can be seen from Figure 7, co-expression of wild type hScrib and PP1γ strongly inhibits the oncogene cooperation between E7 and EJ-ras, whilst the KADA mutant of hScrib is compromised in this activity. These results demonstrate that the hScrib-PP1γ interaction is functionally relevant in an assay of oncogene cooperation.

Discussion

We have shown previously that hScrib can regulate ERK signaling in two ways. The first involves a direct protein interaction, which is mediated via two KIM binding sites located within hScrib. The second appears to involve the recruitment of a protein phosphatase [19]. In this study we provide evidence that a candidate phosphatase is PP1γ. We have also found that hScrib can control PP1γ sub-cellular localisation, with a loss of hScrib promoting PP1γ nuclear translocation.

Regulation of the ERK signaling cascade can occur at multiple levels and can involve Raf dephosphorylation, MEK1,2 phosphorylation, and also MEK1,2 dephosphorylation [24,43–44]. Furthermore, it has been reported that whilst the kinases in the pathway control signal amplitude, the phosphatase PP2A mediates both signal amplitude and signal duration [32–33]. Previous studies have also implicated PP1 in regulating ERK signaling through its ability to dephosphorylate Raf-1 at Ser 259 [45]. Since we have consistently observed that overexpressed hScrib results in a decrease in ERK phosphorylation, we initiated a series of studies to identify the potential phosphatases with which hScrib might interact. Using a proteomic approach we identified PP1γ as a direct interacting partner of hScrib, an interaction that we could confirm both in vitro and in vivo. Analysis of the hScrib amino

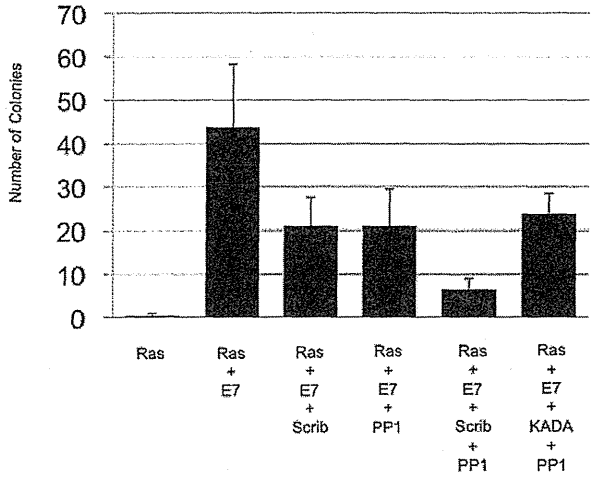

Figure 7. hScrib suppresses HPV-16 E7 and EJ-ras induced transformation in cooperation with PP1γ in a RVxF motif-dependent manner. BRK cells were transfected with EJ-ras alone, HPV-16 E7 plus EJ-ras, HPV-16 E7 plus EJ-ras and wild type hScrib, HPV-16 E7 plus EJ-ras and PP1γ, and HPV-16 E7 plus EJ-ras and wild type hScrib with PP1γ, and HPV-16 E7 plus EJ-ras and PP1γ plus the KADA non-PP1γ binding mutant of hScrib. After three weeks the dishes were fixed and stained and the colonies counted. Results represent the mean number of colonies from 3 independent assays and standard deviations are shown.
doi:10.1371/journal.pone.0053752.g007

acid sequence identified a potential site of interaction, KLDY, mutation of which abolished the ability of hScrib to bind PP1γ. Furthermore, this consensus PP1 recognition motif is conserved in mammalian forms of Scrib, but is absent in Drosophila.

We also analysed the effects of PP1γ ablation upon hScrib control of ERK phosphorylation, and found that loss of PP1γ greatly diminished the ability of hScrib to downregulate the levels of phospho-ERK in vivo. Furthermore, we also found that this activity of hScrib was in part dependent upon an intact PP1γ binding site motif. Interestingly, we also noted that the interaction between PP1γ and hScrib was increased following PKA phosphorylation of hScrib, one potential consequence of which is PP1γ-mediated de-phosphorylation of hScrib. Whether this has an important role with respect to other functions of hScrib remains to be determined and is worthy of further study. Taken together these studies demonstrate that hScrib can interact with PP1γ, an activity which appears to play a role in the ability of hScrib to downregulate the ERK signaling pathway. Interestingly, this regulation of ERK by hScrib has many parallels with a recent study showing that hScrib could also regulate Akt signaling [35]. This required hScrib interaction with the phosphatase, PHLPP1, resulting in the de-phosphorylation of Akt. In this case the interaction between hScrib and PHLPP1 requires sequences in the LRR region of hScrib. Thus hScrib could potentially interact simultaneously with multiple protein phosphatases to control diverse signaling pathways. It should also be emphasized that hScrib is a multifunctional protein, and loss of hScrib also results in increased levels of MEK activity, suggesting multiple mechanisms by which hScrib can control ERK signaling [46].

To investigate whether the capacity of hScrib to interact with PP1γ had any physiological relevance, we made use of an oncogene cooperation assay in primary rodent cells. Previous studies had shown that hScrib could suppress cell transformation induced by HPV-16 E7 and EJ-ras in these cells, and that this activity was dependent in part upon the ability of hScrib to interact with ERK [19]. We reasoned that this activity of hScrib might also be influenced by the ability of hScrib to interact with PP1γ. Indeed, both hScrib and PP1γ, either alone or in combination, could dramatically decrease the levels of HPV-16 E7 and EJ-ras induced cell transformation. However, the additive effects upon the levels of cell transformation, seen with the combination of hScrib and PP1γ, was abolished if a mutant hScrib defective in its ability to interact with PP1γ was included in the assay. This demonstrates that, in the context of an oncogene cooperation assay, the ability of hScrib to interact with PP1γ does play a role in the ability of hScrib to suppress cell transformation.

PP1γ has been linked to the regulation of a variety of different cellular processes, including the DNA damage response, nuclear function and diverse aspects of the cell cycle [47–52]. One of the important aspects of PP1γ regulation is believed to be related to the control of its nuclear expression, which can be mediated by proteins possessing the consensus RVxF PP1 binding motifs, and which can thereby control the correct cellular localization of PP1 [42,52]. We therefore investigated whether hScrib might have a similar potential regulatory function with respect to the pattern of PP1γ localization within the cell. This was indeed found to be the case; in two different assay systems we observed that loss of hScrib resulted in an increased nuclear accumulation of PP1γ, with a concomitant decrease in the levels found in membrane and cytoplasmic fractions. Thus hScrib would appear to contribute directly to the regulation of PP1γ expression patterns. Whether this is related to some of hScrib's previously reported pleiotropic effects upon cell proliferation and cell survival remains to be determined. Taken together, these studies have defined PP1γ as a novel interacting partner of hScrib, an interaction which correlates with hScrib downregulation of ERK signaling and suppression of oncogene-induced cell transformation.

Supporting Information

Figure S1 Schematic diagram showing the different hScrib expression constructs. The schematic shows the arrangement of the functional domains on the hScrib protein, highlighting the LRR, and PDZ domains. The putative PP1-binding site, KLDY is also shown in the carboxy terminal third of hScrib. Also summarized are the results on the interaction assays with PP1γ.
(TIF)

Acknowledgments

We are very grateful to Dr. Mike Myers for his kind support and advice on the proteomic analyses.

Author Contributions

Conceived and designed the experiments: KN LB. Performed the experiments: KN TS AY VKS CK PM MT. Analyzed the data: KN LB. Contributed reagents/materials/analysis tools: KN KK SN TY YT TF SK. Wrote the paper: KN LB.

References

1. Aranda V, Nolan ME, Muthuswamy SK (2008) Par complex in cancer: a regulator of normal cell polarity joins the dark side. Oncogene 27: 6878–6887.
2. Humbert PO, Grzeschik NA, Brumby AM, Galea R, Elsum I, et al. (2008) Control of tumourigenesis by the Scribble/Dlg/Lgl polarity module. Oncogene 27: 6888–6907.

3. Bilder D, Schober M, Perrimon N (2003) Integrated activity of PDZ protein complexes regulates epithelial polarity. Nat Cell Biol 5: 53–58.
4. Thomas M, Narayan N, Pim D, Tomaic V, Massimi P, et al. (2008) Human papillomaviruses, cervical cancer and cell polarity. Oncogene 27: 7018–7030.
5. Navarro C, Nola S, Audebert S, Santoni MJ, Arsanto JP, et al. (2005) Junctional recruitment of mammalian Scribble relies on E-cadherin engagement. Oncogene 24: 4330–4339.
6. Watson RA, Rollason TP, Reynolds GM, Murray PG, Banks L, et al. (2002) Changes in expression of the human homologue of the Drosophila discs large tumour suppressor protein in high-grade premalignant cervical neoplasias. Carcinogenesis 23: 1791–1796.
7. Gardiol D, Zacchi A, Petrera F, Stanta G, Banks L (2006) Human discs large and scrib are localized at the same regions in colon mucosa and changes in their expression patterns are correlated with loss of tissue architecture during malignant progression. Int J Cancer 119: 1285–1290.
8. Bilder D, Li M, Perrimon N (2000) Cooperative regulation of cell polarity and growth by Drosophila tumor suppressors. Science 289: 113–116.
9. Nguyen ML, Nguyen MM, Lee D, Griep AE, Lambert PF (2003) The PDZ ligand domain of the human papillomavirus type 16 E6 protein is required for E6's induction of epithelial hyperplasia in vivo. J Virol 77: 6957–6964.
10. Klezovitch O, Fernandez TE, Tapscott SJ, Vasioukhin V (2004) The PDZ ligand domain of the human papillomavirus type 16 E6 protein is required for E6's induction of epithelial hyperplasia in vivo. Genes Dev 18: 559–571.
11. Vieira V, de la Houssaye G, Lacassagne E, Dufier JL, Jais JP, et al. (2008) Differential regulation of Dlg1, Scrib, and Lgl1 expression in a transgenic mouse model of ocular cancer. Mol Vis 14: 2390–2403.
12. Bilder D (2003) PDZ domain polarity complexes. Curr Biol 13: R661–662.
13. Thomas U, Kim E, Kuhlendahl S, Koh YH, Gundelfinger ED, et al. (1997) Synaptic clustering of the cell adhesion molecule fasciclin II by discs-large and its role in the regulation of presynaptic structure. Neuron 19: 787-799.
14. Dow LE, Brumby AM, Muratore R, Coombe ML, Sedelies KA, et al. (2003) hScrib is a functional homologue of the Drosophila tumour suppressor Scribble. Oncogene 22: 9225–9230.
15. Grifoni D, Garoia F, Schimanski CC, Schmitz G, Laurenti E, et al. (2004) The human protein Hugl-1 substitutes for Drosophila lethal giant larvae tumour suppressor function in vivo. Oncogene 23: 8688–8694.
16. Zhan L, Rosenberg A, Bergami KC, Yu M, Xuan Z, et al. (2008) Deregulation of scribble promotes mammary tumorigenesis and reveals a role for cell polarity in carcinoma. Cell 135: 865–878.
17. Dow LE, Elsum IA, King CL, Kinross KM, Richardson HE, et al. (2008) Loss of human Scribble cooperates with H-Ras to promote cell invasion through deregulation of MAPK signalling. Oncogene 27: 5988–6001.
18. Wu M, Pastor-Pareja JC, Xu T (2010) Interaction between Ras(V12) and scribbled clones induces tumour growth and invasion. Nature 463: 545–548.
19. Nagasaka K, Pim D, Massimi P, Thomas M, Tomaic V, et al. (2010) The cell polarity regulator hScrib controls ERK activation through a KIM site-dependent interaction. Oncogene 29: 5311–5321.
20. Brumby AM, Richardson HE (2003) scribble mutants cooperate with oncogenic Ras or Notch to cause neoplastic overgrowth in Drosophila. EMBO J 22: 5769–5779.
21. Pagliarini RA, Xu T (2003) A genetic screen in Drosophila for metastatic behavior. Science 302: 1227–1231.
22. Yoon S, Seger R (2006) The extracellular signal-regulated kinase: multiple substrates regulate diverse cellular functions. Growth Factors 24: 21–44.
23. Treisman R (1996) Regulation of transcription by MAP kinase cascades. Curr Opin Cell Biol 8: 205–215.
24. Pearson G, Robinson F, Beers Gibson T, Xu BE, Karandikar M, et al. (2001) Mitogen-activated protein (MAP) kinase pathways: regulation and physiological functions. Endocr Rev 22: 153–183.
25. Keyse SM (2000) Protein phosphatases and the regulation of mitogen-activated protein kinase signalling. Curr Opin Cell Biol 12: 186–192.
26. Wang PY, Liu P, Weng J, Sontag E, Anderson RG (2003) A cholesterol-regulated PP2A/HePTP complex with dual specificity ERK1/2 phosphatase activity. EMBO J 22: 2658–2667.
27. Camps M, Nichols A, Gillieron C, Antonsson B, Muda M, et al. (1998) Catalytic activation of the phosphatase MKP-3 by ERK2 mitogen-activated protein kinase. Science 280: 1262–1265.
28. Pulido R, Zuniga A, Ullrich A (1998) PTP-SL and STEP protein tyrosine phosphatases regulate the activation of the extracellular signal-regulated kinases ERK1 and ERK2 by association through a kinase interaction motif. EMBO J 17: 7337–7350.
29. Alessi DR, Gomez N, Moorhead G, Lewis T, Keyse SM, et al. (1995) Inactivation of p42 MAP kinase by protein phosphatase 2A and a protein tyrosine phosphatase, but not CL100, in various cell lines. Curr Biol 5: 283–295.
30. Cohen PT (1997) Novel protein serine/threonine phosphatases: variety is the spice of life. Trends Biochem Sci 22: 245–251.
31. Barton GJ, Cohen PT, Barford D (1994) Conservation analysis and structure prediction of the protein serine/threonine phosphatases. Sequence similarity with diadenosine tetraphosphatase from Escherichia coli suggests homology to the protein phosphatases. Eur J Biochem 220: 225–237.
32. Letourneux C, Rocher G, Porteu F (2006) B56-containing PP2A dephosphorylate ERK and their activity is controlled by the early gene IEX-1 and ERK. EMBO J 25: 727–738.
33. Adams DG, Coffee RL Jr, Zhang H, Pelech S, Strack S, et al. (2005) Positive regulation of Raf1-MEK1/2-ERK1/2 signaling by protein serine/threonine phosphatase 2A holoenzymes. J Biol Chem 280: 42644–42654.
34. Ory S, Zhou M, Conrads TP, Veenstra TD, Morrison DK (2003) Protein phosphatase 2A positively regulates Ras signaling by dephosphorylating KSR1 and Raf-1 on critical 14-3-3 binding sites. Curr Biol 13: 1356–1364.
35. Li X, Yang H, Liu J, Schmidt MD, Gao T (2011) Scribble-mediated membrane targeting of PHLPP1 is required for its negative regulation of Akt. EMBO Rep. 12:818–824.
36. Boukamp P, Petrussevska R, Breitkreutz D, Hornung J, Markham A, et al. (1988). Normal keratinization in a spontaneously immortalized aneuploid human keratinocyte cell line. J Cell Biol 106: 761–771.
37. Graham FL, Smiley J, Russell WC, Nairn R (1977) Characteristics of a human cell line transformed by DNA from human adenovirus type 5. J Gen Virol 36: 59–74.
38. Tomaic V, Gardiol D, Massimi P, Ozbun M, Myers M, et al. (2009) Human and primate tumour viruses use PDZ binding as an evolutionarily conserved mechanism of targeting cell polarity regulators. Oncogene 28: 1–8.
39. Egloff MP, Johnson DF, Moorhead G, Cohen PT, Cohen P, et al. (1997) Structural basis for the recognition of regulatory subunits by the catalytic subunit of protein phosphatase 1. EMBO J 16: 1876–1887.
40. Cohen PT (2002) Protein phosphatase 1-targeted in many directions. J Cell Sci 115: 241–256.
41. Bollen M (2001) Combinatorial control of protein phosphatase-1. Trends Biochem Sci 26: 426–431.
42. Wakula P, Beullens M, Ceulemans H, Stalmans W, Bollen M (2003) Degeneracy and function of the ubiquitous RVXF motif that mediates binding to protein phosphatase-1. J Biol Chem 278: 18817–18823.
43. Tanoue T, Adachi M, Moriguchi T, Nishida E (2000) A conserved docking motif in MAP kinases common to substrates, activators and regulators. Nat Cell Biol 2: 110–116.
44. Dhillon AS, Meikle S, Yazici Z, Eulitz M, Kolch W (2002) Regulation of Raf-1 activation and signalling by dephosphorylation. EMBO J 21: 64–71.
45. Kubicek M, Pacher M, Abraham D, Podar K, Eulitz M, et al. (2002) Dephosphorylation of Ser-259 regulates Raf-1 membrane association. J Biol Chem 277: 7913–7919.
46. Pearson HB, Perez-Mancera PA, Dow LE, Ryan A, Tennstedt P, et al. (2011) SCRIB expression is deregulated in human prostate cancer, and its deficiency in mice promotes prostate neoplasia. J Clin Invest. 121:4257–67.
47. Shimada M, Haruta M, Niida H, Sawamoto K, Nakanishi M (2010) Protein phosphatase 1gamma is responsible for dephosphorylation of histone H3 at Thr 11 after DNA damage. EMBO Rep 11: 883–889.
48. Peng A, Lewellyn AL, Schiemann WP, Maller JL (2010) Repo-man controls a protein phosphatase 1-dependent threshold for DNA damage checkpoint activation. Curr Biol 20: 387–396.
49. Trinkle-Mulcahy L, Andersen J, Lam YW, Moorhead G, Mann M, et al. (2006) Repo-Man recruits PP1 gamma to chromatin and is essential for cell viability. J Cell Biol 172: 679–692.
50. Jiang Y, Luo W, Howe PH (2009) Dab2 stabilizes Axin and attenuates Wnt/beta-catenin signaling by preventing protein phosphatase 1 (PP1)-Axin interactions. Oncogene 28: 2999–3007.
51. Wu JQ, Guo JY, Tang W, Yang CS, Freel CD, et al. (2009) PP1-mediated dephosphorylation of phosphoproteins at mitotic exit is controlled by inhibitor-1 and PP1 phosphorylation. Nat Cell Biol 11: 644–651.
52. Lesage B, Beullens M, Nuytten M, Van Eynde A, Keppens S, et al. (2004) Interactor-mediated nuclear translocation and retention of protein phosphatase-1. J Biol Chem 279: 55978–55984.